Sensitivity of Inflow Determination Techniques for Rotor-Blade Actuator Line Models

R. Boisard, ONERA, Institut Polytechnique de Paris, Meudon, France
S. Péron, ONERA, Institut Polytechnique de Paris, Meudon, France
D. Jude, Analytical Mechanics Associates, Moffett Field, CA, USA
S. Hosseinverdi, Analytical Mechanics Associates, Moffett Field, CA, USA
Jay Sitaraman, U.S. Army Combat Capabilities Development Command, Aviation & Missile Center, Moffett Field, CA, USA

Abstract

As part of a US-France Project Agreement, the US Army and ONERA are investigating mid-fidelity computational approaches for rotorcraft aerodynamics. The approaches from both groups use immersed boundaries instead of boundary-layer-resolved fuselage/hub meshes and actuator lines in the place of rotor blades. The current work focuses on the methodology used in the actuator line model to extract velocities from the background flowfield and the capability of such model to accurately capture Blade Vortex Interactions (BVI). An isolated three bladed rotor is first used to investigate different velocity sampling methods. Following that, an improvement to the actuator line model is explored in order to better capture the tip loads and BVI. In the final application, model improvement is validated on the Dauphin 365N configuration in forward flight.

1. INTRODUCTION

Prediction of aircraft aerodynamics is a key component in the rotorcraft design process. Rotorcraft comprehensive analysis tools, such as RCAS (Ref. 1) and HOST (Ref. 2), are tightly integrated into the design process of a new rotorcraft. However, their aerodynamic models for the rotor, fuselage and rotor/airframe interaction are low-fidelity and often inadequate for complex aerodynamics. At the opposite end of the spectrum from low-fidelity aerodynamic lies high-fidelity, computationally expensive tools using overset Computational Fluid Dynamics (CFD). Frameworks like elsA (Ref. 3) (ONERA) and CREATE™-AV Helios (Refs. 4,5) are established, trusted codes for rotorcraft CFD applications. However complex simulations may take days or weeks to complete.

Research groups at ONERA and the U.S. Army have recently developed mid-fidelity actuator line based methods to accelerate rotor simulations while still using high-fidelity wake capturing techniques from overset CFD methods. The method replaces body-fitted blade meshes with a lifting-line model for each blade.

In recent work presented at the Vertical Flight Society 2024 Forum (Ref. 6), the authors focused on the force injection procedure using various anisotropic Gaussian distributions. In the current work, the other very sensitive part of the actuator line methodology is investigated: the choice of velocity sampling crucial for accurate loads evaluations. A particular focus is made on the ability of actuator line models to capture Blade Vortex Interactions (BVI) which is common in rotorcraft applications.

2. METHODOLOGY

Implementations from both the US Army and ONERA for background Cartesian CFD solvers are based on finite difference formulations of the compressible Navier-Stokes equations using the Spalart-Allmaras (SA) model for turbulence closure. The Cartesian solvers from ONERA (FAST/Cassiopee framework Ref. 11,12) and from US-Army (Helios-Orchard) use octree-based approaches for adaptive mesh refinement. For brevity, this section only describes the actuator line related methodologies. More detailed information about the Cartesian solvers can be found in previous work on Orchard (Ref. 4,5) and FAST/Cassiopee (Ref. 13,14).

Some high-fidelity results are included in this work to provide a baseline for comparing accuracy of mid-fidelity models. High-fidelity results in this work were obtained either using Helios-Rapidus (Ref 9) and are labeled as Helios in the figures, or using FAST/Cassiopee frameworks and are labeled as FAST in the figures.

2.1. Actuator line model

RotorROM (ONERA) and ROAM (US-Army) have very similar actuator line methodologies using nonisotropic Gaussian distributions to inject loads into the background Cartesian mesh. (Eq.(1)). The Gaussian widths in each direction are described using ε_c, ε_r, and ε_n for the chord-wise, radial, and normal directions respectively.

(1) $$g(x_c, x_n, x_r) = \frac{1}{\varepsilon_c \varepsilon_n \varepsilon_r \pi^{3/2}} exp\left(-\frac{(P_c - x_c)^2}{{\varepsilon_c}^2} - \frac{(P_n - x_n)^2}{{\varepsilon_n}^2} - \frac{(P_r - x_r)^2}{{\varepsilon_r}^2}\right)$$

The actuator line process can roughly be reduced to three steps:

1. Estimate a local angle-of-attack using blade dynamics and velocity field from the flow-field in the surrounding Cartesian mesh.
2. Use the angle-of-attack to compute sectional loads using airfoil tables and, eventually, apply corrections (3D tip-losses, compressibility, etc.).
3. Inject the sectional loads as source terms in the governing Navier–Stokes equations discretized in the background Cartesian mesh.

RotorROM and ROAM, mainly differ in the default behavior of step 1. In RotorROM, the same Gaussian weights used for injection are used to extract inflow for each blade section, based on the work of Churchfield et. al. (Ref. 10). Helios ROAM does not use the Gaussian weights directly to estimate the inflow because the weights ROAM uses are approximate and do not guarantee to integrate to unity. Traditionally ROAM has instead relied upon a "circle-of-sensors" approach to extract the flow velocity. The "circle-of-sensors" approach uses 30-60 points in a circle around each blade section and averages the flowfield over those points to estimate inflow while canceling the effect of bound circulation. In both solvers the field velocities are then combined with the local blade dynamics into an angle-of-attack and used through aerodynamic look-up tables to extract blade loads.

For the current study, different velocity sampling methods were added to both solvers in order to investigate their effects on the extracted angle of attacks that dictate the radial load distributions.

2.2. Lifting-Line Correction

Step (1) from the previous section does not always produce an accurate angle-of-attack, especially in regions of 3-dimensional flow. As such a lifting-line-based correction was developed as part of this work to improve the angle-of-attack estimation.

Lifting-line theory is commonly used as a low-order approximation to aerodynamics for wings or rotating blades. The control points for lifting-line theory are the 3/4 chord in order to satisfy the Kutta-condition. Figure 1 shows a common lifting-line model applied to a rotating blade; each j^{th} panel has associated with it a bound circulation, Γ_j. Trailed circulation is a result of changes in lift from panel-to-panel and the trailed wake is assumed in this diagram to be planar and trail the direction of rotation.

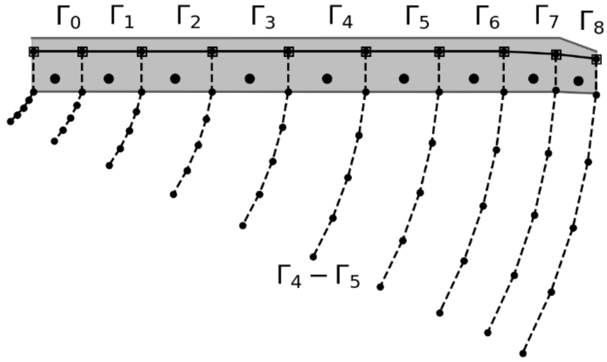

Figure 1: Lifting-line model of a rotor blade showing bound and trailed circulation for 9 panels.

Without a flow-field from CFD, lifting-line theory attempts to solve a no-flux boundary condition at the blade control points, described mathematically as:

$$\left(\overrightarrow{V_B} + \overrightarrow{V_T}\right) \cdot \hat{n} + V_\infty sin(\alpha) = 0$$

where $\overrightarrow{V_B}$ is the induced velocity at a panel from all contributions of bound circulation and $\overrightarrow{V_T}$ is the induced velocity at a panel from all contributions of trailed circulation and α is the local 2D angle of attack. Velocity contribution from circulation distributions of the finite vortex system above can be expressed as a summation of individual segment contributions that are obtained from the Biot-Savart law:

$$\overrightarrow{V_i} = \sum_{j}^{nseg} \Gamma_j \int_0^{l_j} \frac{\overrightarrow{dl} \times \overrightarrow{r_{ij}}}{\left|r_{ij}\right|^3}$$

where Γ_j represents the strength of the j^{th} vortex filament (segment), r_{ij} is the vectorial displacement of the i^{th} control point with respect to the j^{th} filament, and l_j is the vector of the filament itself.

The velocity at each control point is a linear combination of the circulations on the blade resulting in a system of equations:

$$[A_{ij}][\Gamma_j] = -V_n$$

where $[\mathrm{A}]$ is a matrix of summed contributions from the bound, $[\mathrm{B}]$, and trailed, $[\mathrm{T}]$, circulations. $[\mathrm{B}]$ and $[\mathrm{T}]$ can be constructed explicitly for a blade. The system of equations, which is a dense square matrix, are then solved for Γ.

In the case of actuator lines used with a CFD background mesh, there is an "observed" normal velocity already extracted from the flow-field. The observed velocity is obtained in a way that accounts for the bound circulation of the vortex along the 1/4-chord of the blade but perhaps, per the authors' hypothesis, does not fully account for the trailed contribution. Given an observed normal velocity, the system of equations is solved such that Γ is known over the blade. A corrected normal velocity, $\widehat{\mathrm{V}_{\mathrm{n}}}$, is proposed such that:

$$\widehat{V_n} = V_n + [T_{ij}][\Gamma_j] = -[B_{ij}][\Gamma_j]$$

The corrected normal velocity is used along with the chord-wise velocity to obtain the Mach number and angle of attack for 2D table look-up. In regions of the blade where there is little gradient in lift (i.e. mid-span), trailed vorticity is small and the correction is minimal.

In the model illustrated in Figure 1, five vortex segments are used for the trailed wake over 30°. However, the number of vortex segments and wake geometry are empirical. The simplest form of a trailed wake model would be to only use the first trailed vortex segment spanning from the 1/4 chord to the trailing edge of the blade.

2.3. TEST CASES

This study relies on two different test cases.

The first one is the Dauphin D365N in forward flight that was already used in the previous studies to verify actuator line implementation and to study the effect of the force injection procedure (Ref. 6). This model has 4 blades with a radius of 0.75 meter, 12 degrees of linear twist and uses OA209 airfoils. The rotor control angles and response (collective, flap, lag and harmonics) are obtained from the rotorcraft comprehensive code HOST (Ref. 2). Rigid blade deflections are applied about lag and flap hinges using three harmonics. In experiments the D365N configuration was trimmed to a specific thrust ($\bar{Z} = 14.5$), axial force ($\bar{X} = 0$) and zero rotor lateral flapping. The baseline flow conditions are $V_\infty = 15 m.s^{-1}$, corresponding to a moderate advance ratio of $\mu = 0.15$, -3° fuselage angle-of-attack and zero side-slip. This test case features strong blade vortex interactions which make it of greath interest for this study.

The second test case is a more academic one. It is an isolated three bladed rotor in hovering conditions. Rotor blades are 8.97m radius with naca0012 cross section and 15° linear twist. Blade pitch was set to 10° and rotor is considered fully rigid with neither flap nor lead-lag articulations. In these conditions the flowfield features mild blade vortex interactions making this test case interesting for testing the different velocity sampling methods and BVI correction for actuator line.

3. RESULTS

3.1. STATUS ON ACTUATOR LINE ACCURACY

The dauphin D365N test case was used to validate RotorROM and ROAM actuator line modules. Loads injection is performed using the function described in 2.1 and velocity sampling is done using the same kernel function. No lifting line correction was applied in those computations.

Figure 2 shows a comparison in terms of rotor thrust with respect to blade azimuth between FAST solver (body fitted blades) and the two actuator line solvers on the Dauphin D365N test case. It can be observed that load fluctuations predicted by the actuator line models show good agreement with corresponding data from the blade solved simulation. In terms of absolute values, discrepancies are of the order of 7% of the loads, with an overestimation for both RotorROM and ROAM. This level of accuracy is consistent with the accuracy of lifting line / freewake methods, which relies on the same 2D airfoil datas hypothesis, and also acceptable knowing the gain in computational cost compared to bodyfitted computations.

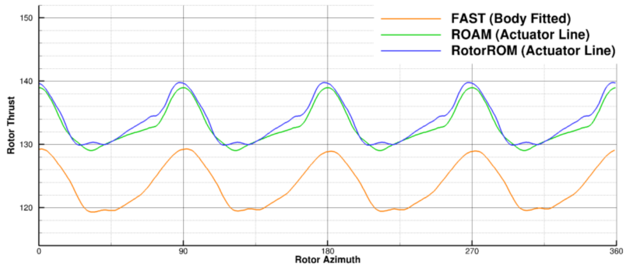

Figure 2: Integrated rotor thrust (in N) for the Dauphin D365N test case

Figure 3 is showing a comparison in terms of the time averaged fuselage center line pressure between FAST solver (body fitted blades) and both actuator line methods. Actuator line performed very well at capturing the interaction between the fuselage and the rotor wake. There is almost no difference in the fuselage pressure centerline between the body fitted computation (FAST) and actuator line models.

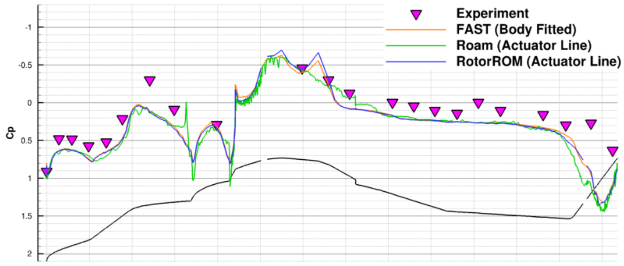

Figure 3: Time average pressure at fuselage center line for the Dauphin D365N test case

According to these results, actuator line models can be seen as reasonably accurate, CPU efficient methods for rotorcraft applications since they are able to capture both the rotor loads and the wake interactions, which is not possible with lower fidelity methods.

However, limiting the comparison to integrated loads may not be sufficient for some applications, and could hide non-physical azimuthal or radial loads signature. A more detailed view of the blade spanwise load distribution is shown in Figure 4 for three different blade azimuths. At azimuth 0° (blade align toward the back of the rotorcraft) there is a very good match between actuator lines model and body fitted computation. The small blade vortex interaction occurring around 45% blade span is also captured with only minor discrepancies in terms of position and amplitude. But, at azimuth 90° and 180°, were strong BVI occurs, it can be observed that, important discrepancies occur near the BVI location. The two actuator line results feature larges overestimations of the interactions, with also some slight phase shift along the span on ROAM computation. These differences may be due to the use in ROAM, of a tip loss function. Since classical tip loss function from the literature like Prandtl one cannot be applied to a helicopter rotor with a freestream flow almost tangent to the rotor disc, a simple forcing of the loads toward zero is applied from 95% of the blade span. Therefore, this tip loss correction relies on very few physical meanings and does not lead to a significant improvement of the load distribution along with a potential shift of the vortex emission position.

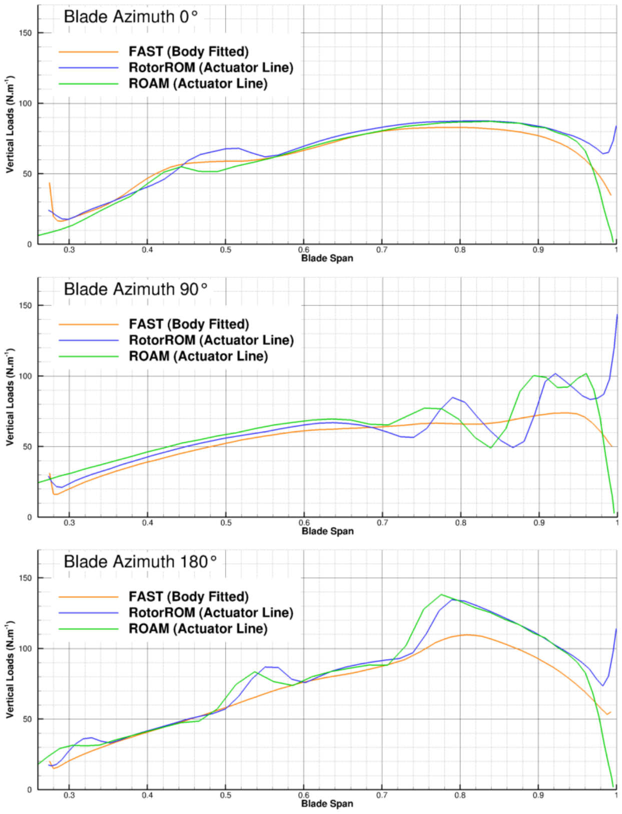

Figure 4: Spanwise distribution of loads on the Dauphin D365N test case at blade azimuth 0° (top) azimuth 90° (middle) and 180° (bottom)

This observation of the overestimation of loads in BVI region, characterized by non-negligible spanwise velocities because of the strong cross flow, motivated the parametric study of velocity sampling methods performed in the next section. It was conjectured that a carefully selected choice of the velocity sampling function may improve the evaluation of the velocities and therefore the angle of attack and hence improve the load prediction.

3.2. VELOCITY SAMPLING PARAMETRIC STUDY

Based on the issue identified in BVI conditions, a velocity sampling study was performed using the hovering case of the three bladed NACA0012 rotor which is a simpler test case and should be easier to analyze.

To avoid the coupling between the velocity sampling methods and the loads application method, a “prescribed” actuator line method was implemented. In this approach, a first computation is performed using Helios-Rapidus solver with body fitted rotor blades for 21 revolutions. Once the computation has converged, spanwise distribution of loads is extracted. Since it is an isolated rotor in hover condition, only the last iteration is sufficient to rebuild the full rotor loads. Following this first step, blade loading from the body fitted computation is prescribed in the actuator line model. The prescribed actuator line computation using ROAM and RotorROM is then performed for at least 10 revolutions in order to fully develop the rotor wake. The Gauss parameters used to spread the momentum sources were chosen using the best practices identified in previous studies from the authors (Ref. 6) namely 40% chord in the chordwise direction and 25% chords in the normal direction.

Figure 5 is showing the rotor wake from both actuator line models on top of Helios-Rapidus computation.

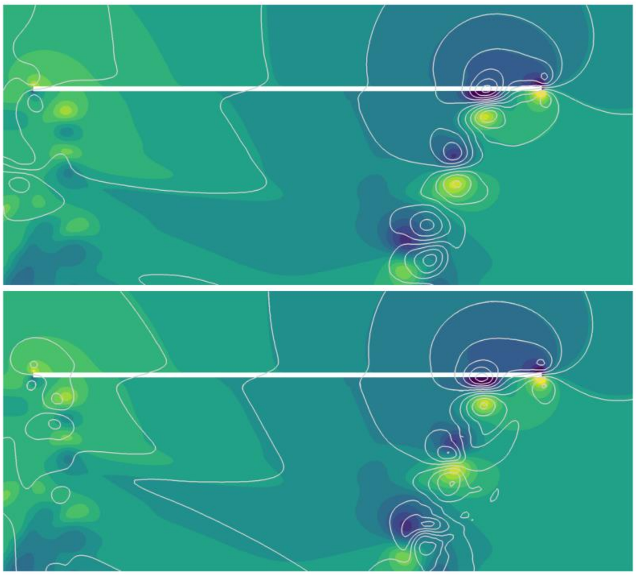

Figure 5: Comparison of wake structure between body fitted computation (background) and prescribed actuator line models (lines) using ROAM (top) and RotorROM (bottom)

The overall wake structure is very similar between both actuator line models and body fitted computation. Tip vortices at the root are less intense in the actuator line computation due to a coarser discretization of the actuator line in this area. Near the tip, vortices are emitted at the correct position and blade vortex interaction also occurs at the right position around 90% blade span. Older vortices suffer from a slight shift in position between the computation. This is due to the lake of actual blade walls in the actuator line model, which does not lead to a bursting of the vortices as it is the case in Rapidus computation. This also affects the flowfield close to the blade vortex interaction on the upper part of the rotor disc. After one rotor revolution of wake age, more deviations can be observed between RotorROM and Rapidus computations. Those discrepancies are mainly due to the propagation of the wake by the CFD solvers. The cartesian background grid solver used in ROAM is the same as the one used for body fitted computation which is not the case for RotorROM actuator line. Overall, it can be considered that wakes developments are sufficiently similar between prescribed actuator line and body fitted blades computations, to use this flow solution as a starting point to evaluate different velocity sampling methods.

From this flow solution, a large variety of velocity sensors shape were used to extract local velocities and compute the loads that would have been applied using these specific sensors. Several hundreds of sensors shapes were used, varying the number of sensor points and the distance between the actuator line point and sensors (illustrations of different shapes are given in Figure 6):

- ✓ The gaussian function used for load injections (denoted in the following figures as Gauss method)
- ✓ A unique point located at the center of the gauss injection function (denoted as point method)
- ✓ Some two-dimensional shape like squares, rectangles, circles or ellipses
- ✓ Three dimensional shapes like spheres or ellipsoids
- ✓ Extractions on a plane perpendicular to the blade with different weighted averaging

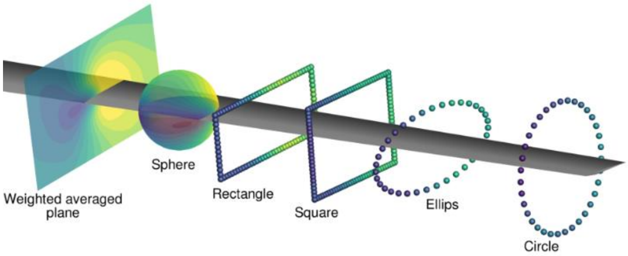

Figure 6: Different sensors shapes used for velocity sampling

Figure 7 is showing a comparison between the prescribed loads (from rotor blades body fitted computations) and the loads that would have been applied using the velocity sampling from different kind of sensors shapes. It can be observed that up to 80% radius, all the velocity sampling methods show almost perfect match in terms of loading. There is no effect of the distance between the sampling points and the actuator line point. It means that any closed surface is actually able to accurately capture the velocity field around the airfoil outside of a vortex region. At the blade tip, it can also be observed for all methods that the loads are not going back to zero. It is due to the fact that no tip loss function was used, and therefore such behavior is expected from an actuator line model.

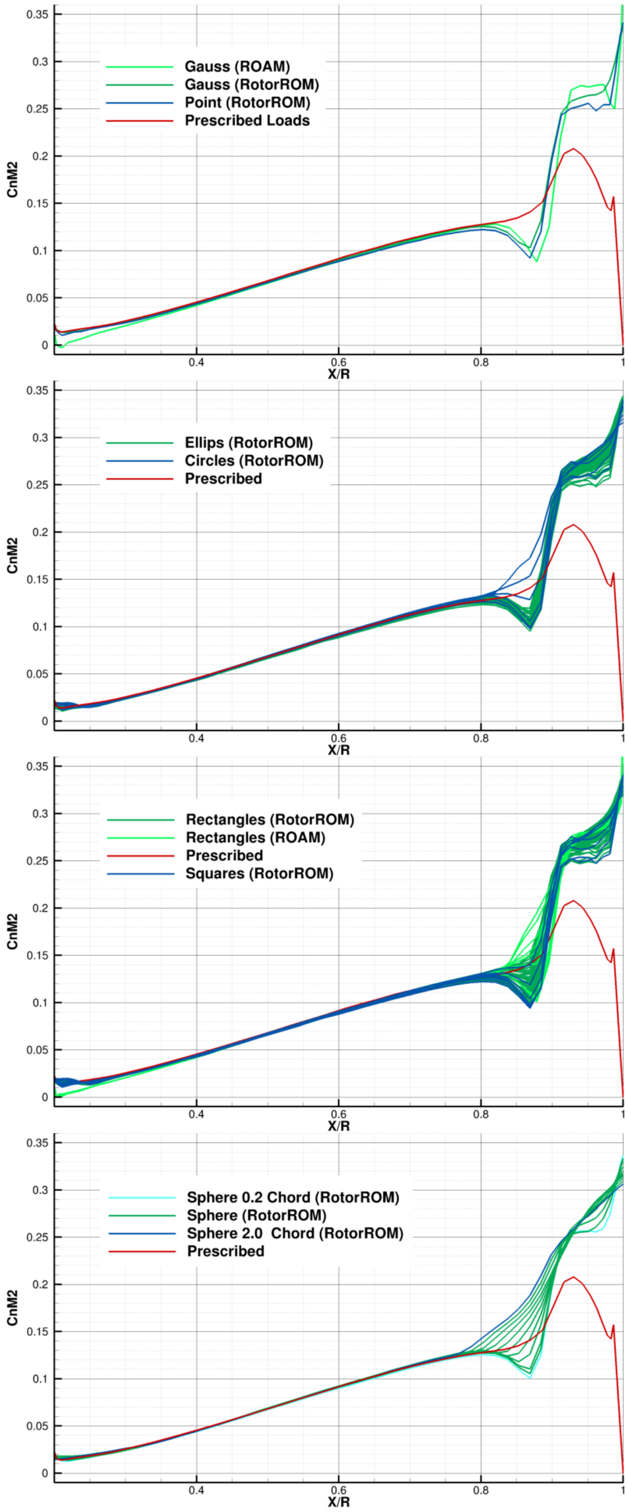

Figure 7: Comparison between prescribed loads and loads computed using various velocity sampling method

In the region where the blade is intersecting the previous blade tip vortex, Gauss and point methods are giving very similar results with a strong loss of loads inboard of the vortex path, compensated by a strong gain in loads outboard. Small differences appear between RotorROM and ROAM Gauss method due to the fact that in ROAM, only the two-dimensional part of the Gauss function aligned with the blade section is used, while in RotorROM, the full 3D Gauss function is used. The loads computed using these sampling methods are also very similar to the one obtained using other sensor shapes with very small distance between the sensors and the actuator line point.

Using rectangles, ellipses or spheres seems to gives the opportunity to remove the undershoot of loads on the inboard part of the vortex path. However, in order to match as close as possible the prescribed load in this area, the sampling distance from the actuator line point has to be carefully chosen. Moreover, the overshoot of loads on the outboard part is then increased. A closer look at the flowfield in the vicinity of the velocity sensors in this area can give some insight of the phenomenon involved.

Figure 8 is showing the spanwise distribution of angle of attack along the blade using circle sensors and Figure 9 is giving a closer view of the vertical velocity at three different radial stations along with the positions of the circle velocity sensors. The vertical velocity is directly linked to the normal induced velocity and therefore linked to the local angle of attack which is responsible for the blade loading in the actuator line model.

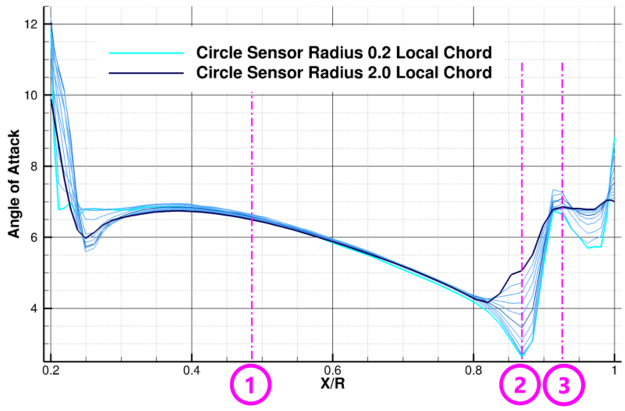

Figure 8: Spanwise distribution of angle of attack using circles sampling method

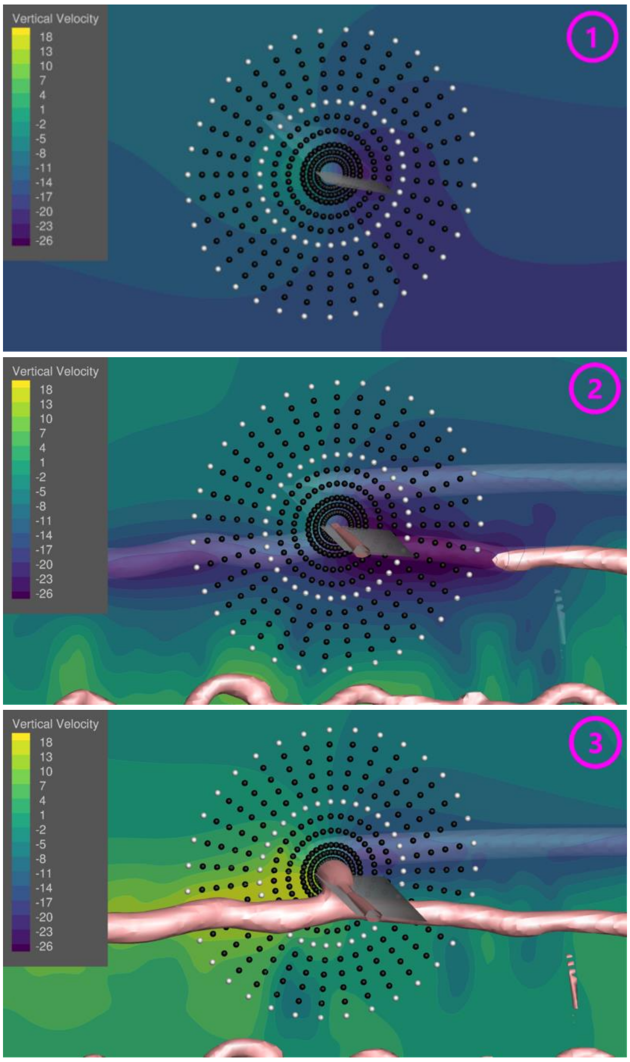

Figure 9: Detailed view of normal induced velocity in the vicinity of the BVI

At position (1) far from the tip vortex interactions, the flow around the actuator line point does not feature any strong fluctuation, and is relatively homogeneous in all the direction. Therefore, for any sensors circle radius, the spatial averaging of velocities will give very similar values, hence there is no effect of the circle's radius on the angle of attack and the loads. At position (2), inboard of the tip vortex interaction, there is some strong fluctuation of the velocities in the vicinity of the actuator line point due to the proximity of older tip vortices. Extending the sensors circle radius up to one or two chords will induce a velocity sampling in the area of influence of older tip vortices below the rotor disc. It is actually the overestimation of the older tip vortex influence that lead to a reduction of the normal velocity (hence angle of attack and loads undershoot) evaluated using sensors circles with radius above 0.7 chord. Not only the apparent improvement of the loads estimation is therefore linked to a non-physical overestimation of these vortices influence, but it also makes the computed velocity highly dependent on the sensors circle radius and the test case. At position (3), outboard of the tip vortex interaction, the flow is less contaminated by older vortices due to wake contraction. Therefore, velocity evaluation is less sensitive to the sensors circle radius. Increasing the circle radius will nonetheless overestimate the effect of these vortices at the local actuator line point leading to a nonrealistic estimation of the angle of attack.

As a conclusion, even if the circles of sensors seem to show better agreement inboard of the tip vortex path for a carefully chosen radius, it is not for physical reason but only due to error compensation. Moreover, this type of sampling is highly dependent of the distance between the sensors and the actuator line point and no clear rule to choose this distance can be established. In case of blade vortex interaction, the more accurate distance between sensors and actuator line points will depend on the location of older vortices hence on the rotor and flight conditions. Therefore, it seems not advisable to use any form of sensors that will be "too far" from the actuator line point. As a matter of fact, using the Gaussian projection function used to apply the loads for the velocity sampling seems to be the best option, avoiding any tuning parameters that could be misleading in the interpretation of the results even if it does not solve the issue in estimating the loads near blade vortex interaction. Point sensors could also appear as a good option for the same reason, however, it has shown some strong instabilities in specific cases.

3.3. EFFECT OF LIFTING LINE CORRECTION

Observations from 3.2 clearly show that tuning the velocity sampling method is not the right way to proceed in order to improve actuator line model in the vicinity of vortices. This leads authors to consider the correction based on lifting line method described in 2.2 and relying on $\widehat{V_n}$.

A first test of the lifting line correction was performed using the same test case as the one used for velocity sampling parametric study. As advised in 3.2 the Gaussian function was used for velocity extraction from the flowfield. Figure 10 is showing a comparison of the normal and chordwise sectional load estimation with and without correction. It can be observed that below 80% of the blade span, the correction does not lead to any modification of the loads. This mean that this correction is self-limited to the region of cross-flow. Around 90% blade radius, where the blade vortex interaction is occurring, there is a strong damping of the loads' fluctuations both inboard and outboard of the tip vortex position for both lifting line methods. It features a very good phasing with respect to the prescribed loads in terms of position of the minimum and maximum of the fluctuations. The amplitude of the fluctuation is also well predicted for the normal force. Larger discrepancies still appear on the chordwise load, there is nonetheless a great improvement compared to the computations without correction. Moreover, chordwise loads are quite small, hence their contribution to the total loads is small and are also known to be more difficult to capture than the normal one using 2D airfoil tables. It can also be observed that, in the tip region, all the loads are naturally decreasing to a value close to zero without any need of adding a tip loss function.

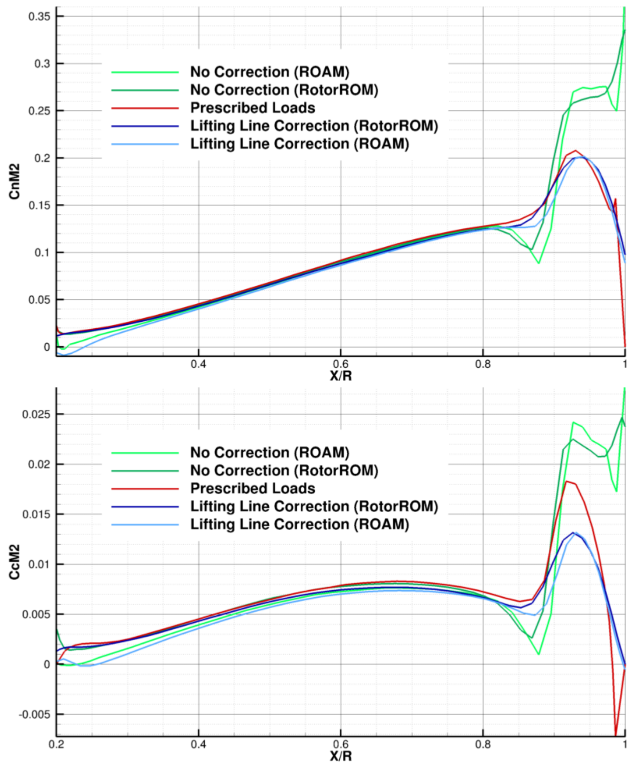

Figure 10: Effect of lifting line correction on normal (top) and chordwise sectional loads (bottom)

There are a few tuning parameters investigated for this test case. The first is the core radius size for the wake trailers, which can be freely chosen at runtime and affects damping of the loads' fluctuations in spanwise velocities gradient regions. In the present study, its value was chosen based on empirical considerations. The second tuning parameter investigated in this work is the number of wake trailers. For results in Figure 10 only a single wake trailer was used. From Figure 1, using only the first wake trailer is the simplest approximation of the near-wake effects and does not depend on assumptions about the wake geometry.

Based on the improvement observed on the simple test case of the NACA0012 rotor, the correction was applied to the D365N test case shown in section 3.1. RotorROM was again tested with a single wake trailer whereas ROAM was tested with both single and 8-segment trailers.

Effect of the lifting line correction on spanwise distribution of loads is shown on Figure 11. At blade azimuth 0°, where there is almost no blade vortex interaction, it can be observed that the main effect of the lifting line correction is to lower the loads near the tip, producing a closer match with the body fitted computation. At azimuth 90° and 180°, where strong BVI occurs, RotorROM shows a dampened signal as a result of the correction. ROAM, however, with only 1 trailer does not show the same damped result as RotorROM. With 8 trailers, ROAM shows better agreement with FAST. The level of fluctuations from the body fitted computation are not perfectly recovered, but it nonetheless leads to an important improvement. For both azimuths, the tip loads are also perfectly recovered when the correction is used.

As seen in Figure 12, the improvement of the spanwise loads leads also to an improvement on the rotor integrated loads. The RotorROM actuator line model using lifting line correction almost perfectly match the loads obtains by the body fitted computation. For ROAM, again 8 wake segments were needed instead of 1 to better match results from FAST. The overestimation that was observed without correction was mainly due to the overestimation of loads at the tip of the blade.

A detail of note for this case is that ROAM and RotorROM are not using the same airfoil tables for forces and moments. This could explain some of the discrepancies, especially in integrated loads between both solvers. ROAM also uses a different Gaussian sampling weights compared to RotorROM, which may have an effect on the perceived normal velocity.

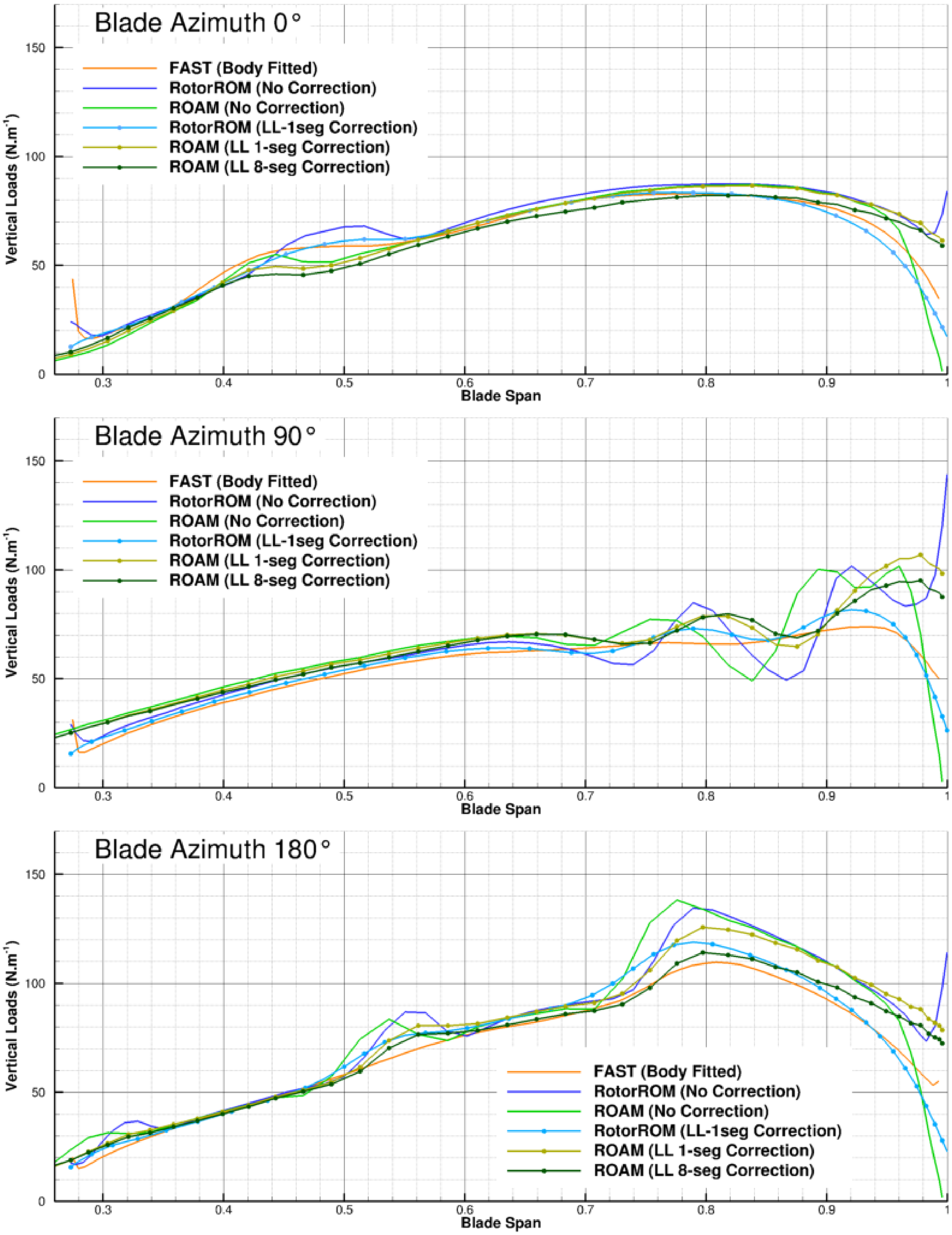

Figure 11: Spanwise distribution of loads on the Dauphin D365N test case at blade azimuth 0° (top) azimuth 90° (middle) and 180° (bottom) with and without lifting line correction

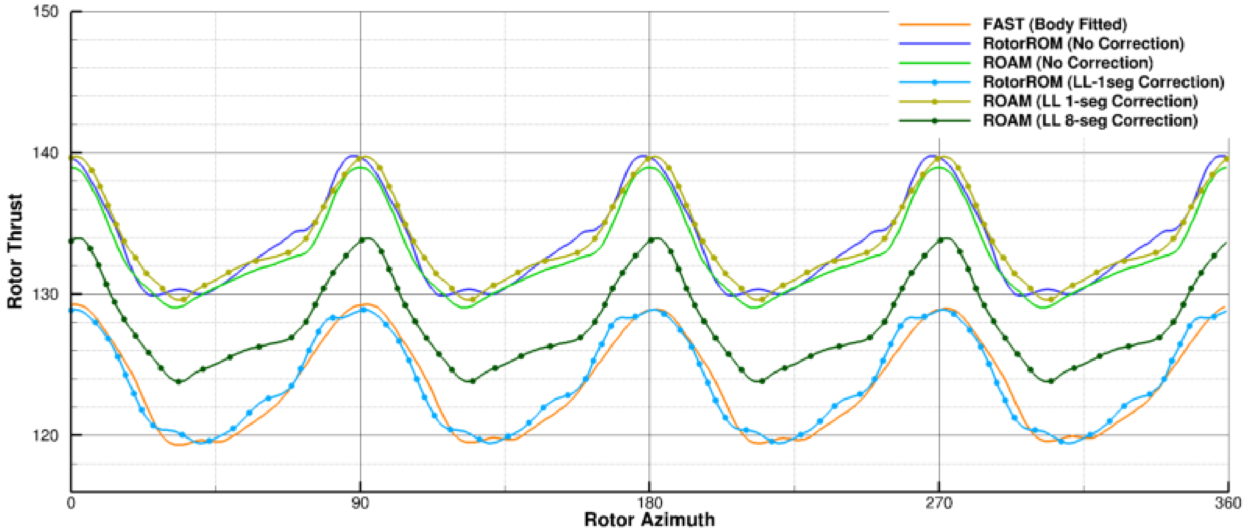

Figure 12: Integrated rotor thrust (in N) for the Dauphin D365N test case

4. CONCLUSIONS

In this study it was shown that actuator line methods are very good alternative to more expensive blades body fitted computation to evaluate rotor loads and wake interactions. However, it was outlined that the interpretation of the rotor integrated loads could hide some important discrepancies in the spanwise load distribution, especially in the vicinity of blade vortex integration.

The velocity sampling methods, which could at first be seen as a way to mitigate the discrepancies observed in BVI region. However, improvement is linked to error compensation and no generic choice of sensors size can be identified. To overcome this issue, the authors suggest to use the Gauss projection from the application of the loads also for the velocity sampling. If it cannot be done, then distance between the center of the actuator line points and the velocity sensors should be kept small enough to not overestimate the velocities induced from older vortices on the actuator line points.

A new methodology based on a near wake correction was introduced in order to reduce fluctuations from blade vortex interactions. For advancing rotor, where Prandtl-type tip loss correction is not applicable, this approach also enables to avoid the use of arbitrary forcing function to decrease the tip loads to zero. This new correction was successfully applied on the NACA0012 rotor and the D365N in advancing flight conditions. In both cases, the same implementation of the correction function was able to largely improve the spanwise distribution of load in the BVI region and also the natural decrease of the loads near the blade tip.

Future work should be considered to further investigate discrepancies between RotorROM and ROAM for the near wake correction. Whereas RotorROM showed diffused BVI with only a single wake trailer, ROAM needed additional trailers to dampen load variations.

5. ACKNOWLEDGMENTS

The authors would like to acknowledge the U.S./France Project Agreement on Rotary-Wing Aeromechanics and Human Factors Integration Research, a longstanding cooperation between the U.S. Army, ONERA and DGA. Material presented in this work is a product of the CREATE (Computational Research and Engineering for Acquisition Tools and Environments) element of the U.S. Department of Defense HPC Modernization Program. Support was also provided by the US Army Combat Capabilities Development Directorate Aviation & Missile Center.

6. REFERENCES

1. Saberi, H., Hasbun, M., Hong, J., Yeo, H., and Ormiston, R., "RCAS Overview of Capabilities, Validations, and Applications to Rotorcraft Problems," American Helicopter Society 71st Annual Forum Proceedings, Virginia Beach, VA, 2015.
2. Benoit, B., Kampa, K., von Grunhagen, W., Basset, P.-M., and Gimonet, B., "HOST, a general helicopter simulation tool for Germany and

France," Annual Forum Proceedings-American Helicopter Society, Vol. 56, 2000.

3. Cambier, L., Heib, S., and Plot, S., "The ONERA elsA CFD software: input from research and feedback from industry," Mechanics & Industry, Vol. 14, (03), 2013, pp. 159–174.

4. Wissink, A. M., Jude, D., Jayaraman, B., Roget, B., Lakshminarayan, V. K., Sitaraman, J., Bauer, A. C., Forsythe, J. R., and Trigg, R. D., "New Capabilities in CREATE-AV Helios Version 11," AIAA SciTech 2021 Forum, Jan 2021.

5. Jude, D., Sitaraman, J., andWissink, A., "An Octree-Based, Cartesian Navier-Stokes Solver for Modern Cluster Architectures," J. Supercomput., Vol. 78, (9), jun 2022, pp. 11409–11440. DOI: 10.1007/s11227-022-04324-7.

6. Jude, D., Hosseinverdi, S., Sitaraman, J., Péron, S., and Boisard, R., "Actuator Line and Immersed Boundary Methods for Rotorcraft CFD", VFS Forum, Vertical Flight Society, May 2025.

7. Lakshminarayan, V. K., Sitaraman, J., Roget, B., and Wissink, A. M., "Development and validation of a multi-strand solver for complex aerodynamic flows," Computers & Fluids, Vol. 147, 2017, pp. 41–62.

8. McDaniel, D. R., Tuckey, T., and Morton, S. A., The HPCMP CREATE™-AV Kestrel Computational Environment and its Relation to NASAs CFD Vision 2030. DOI: 10.2514/6.2017-0813.

9. S. Hosseinverdi, J. Sitaraman, D. Jude, P. Premaratne, L. Erlandson, and D. Appelhans, "Rapidus: Performance-Portable Parallel Flow Solver for Aerospace Applications," AIAA SCITECH 2025 Forum. American Institute of Aeronautics and Astronautics, Jan. 03, 2025. doi: 10.2514/6.2025-1484.

10. Churchfield, M. J., Schreck, S. J., Martinez, L. A., Meneveau, C., and Spalart, P. R., "An Advanced Actuator Line Method for Wind Energy Applications and Beyond," 35th Wind Energy Symposium, Jan 2017. DOI: 10.2514/6.2017-1998.

11. https://github.com/onera/Cassiopee

12. https://github.com/onera/Fast

13. Péron, S., Benoit, C., Renaud, T., Mary, I., "An immersed boundary method on Cartesian adaptive grids for the simulation of compressible flows around arbitrary geometries", Engineering with Computers 37, 2419–2437 (2021). https://doi.org/10.1007/s00366-020-00950-y

14. Suss, A., Mary, I., Le Garrec, T., Marié, S., "Comprehensive comparison between the lattice Boltzmann and Navier–Stokes methods for aerodynamic and aeroacoustic applications", Computers & Fluids, vol. 257, 2023. https://doi.org/10.1016/j.compfluid.2023.105881.